Ionic Blockage of Sodium Channels in Nerve

ANN M. WOODHULL

From the Department of Physiology and Biophysics, University of Washington School of Medicine, Seattle, Washington 98195. Dr. Woodhull's present address is Hampshire College, Amherst, Massachusetts 01002.

ABSTRACT   Increasing the hydrogen ion concentration of the bathing medium reversibly depresses the sodium permeability of voltage-clamped frog nerves. The depression depends on membrane voltage: changing from pH 7 to pH 5 causes a 60% reduction in sodium permeability at +20 mV, but only a 20% reduction at +180 mV. This voltage-dependent block of sodium channels by hydrogen ions is explained by assuming that hydrogen ions enter the open sodium channel and bind there, preventing sodium ion passage. The voltage dependence arises because the binding site is assumed to lie far enough across the membrane for bound ions to be affected by part of the potential difference across the membrane. Equations are derived for the general case where the blocking ion enters the channel from either side of the membrane. For H^+ ion blockage, a simpler model, in which H^+ enters the channel only from the bathing medium, is found to be sufficient. The dissociation constant of H^+ ions from the channel site, 3.9×10^{-6} M (pK_a 5.4), is like that of a carboxylic acid. From the voltage dependence of the block, this acid site is about one-quarter of the way across the membrane potential from the outside. In addition to blocking as described by the model, hydrogen ions also shift the responses of sodium channel "gates" to voltage, probably by altering the surface potential of the nerve. Evidence for voltage-dependent blockage by calcium ions is also presented.

Hydrogen ions decrease the sodium currents that are responsible for nerve action potentials. The effects of H^+ ions on sodium permeability are said to be similar to the titration of an acid: the more H^+ ions are added to the bathing medium, the less sodium permeability remains (Hille, 1968; Drouin and The, 1969).

The new finding presented in this paper is that a given concentration of H^+ ions blocks sodium currents more or less, depending upon the potential across the nerve membrane. A simple theory for how this can happen is that the H^+ ion may enter the sodium channel and bind there, preventing the passage of sodium ions. Being inside the membrane, the H^+ ion would respond to membrane voltage.

A kinetic model for ionic blockage of channels is developed here. The applicability of this model to the data for H^+ blockage of sodium channels

and the values of the model's parameters provide new information about the inside of the sodium channel. The information accords well with the idea that there is an acidic group inside the sodium channel.

METHODS

Nodes of Ranvier of single myelinated nerve fibers from the frog, *Rana pipiens*, were voltage clamped by the method of Dodge and Frankenhaeuser (1958). Refinements incorporated in the voltage clamp used here are given in Hille (1971). All nodes were held at −80 mV. (Membrane potential is defined as outside minus inside potential. Outward current is positive.) Before each test pulse, the node was hyperpolarized to about −125 mV for 40 ms to remove sodium inactivation.

Recording and Analysis

Oscilloscope traces of current vs. time were recorded on film after the leakage and capacity currents had been subtracted electronically. The leakage and capacity subtractors were adjusted to cancel the currents produced by a hyperpolarizing pulse (Armstrong and Hille, 1972). The leakage current of nodes is linear from −80 to +80 mV at pH 7 (Hille, 1967, Fig. 5). Nodes that required no capacity current subtraction gave the same results as those for which the subtraction was made. The peak values of sodium current were read off by eye from film records projected onto a grid. Graphs of peak current vs. voltage in normal Ringer and in Ringer with $\frac{1}{8}$ the normal sodium concentration were used to calculate the attenuation artifact (Dodge and Frankenhaeuser, 1958; Hille, 1971). The attenuation artifact averaged 24% ($\pm 10\%$ SD) in nine experiments. All voltages given in this paper are corrected for this attenuation; the average factor was used in the few experiments in which the factor was not measured.

Recorded currents were converted to nanoamperes by assuming that the resting resistance of the node was 40 MΩ in normal Ringer solution. The Goldman-Hodgkin-Katz flux equation, which is appropriate for sodium currents in frog nodes, was used to calculate sodium permeabilities from currents (Goldman, 1943; Hodgkin and Katz, 1949; Dodge and Frankenhaeuser, 1959).

General Procedure

The chamber with the nerve fiber was put into a brass enclosure maintained at 5°C, and was allowed to equilibrate for 20 min. After equilibration, the first voltage clamp series was taken in Ringer solution. Then the solutions were changed in quick succession, 2 or 3 min in each solution being sufficient for a voltage clamp series. For each solution change 10–20 vol of solution were exchanged. Before and after each test solution came a control voltage clamp series in Ringer or another standard solution for comparison. When analysis showed a pair of controls to be very different, the data for the test solution between them were discarded.

Solutions

The compositions of the bathing solutions surrounding the node under study are given in Table I. Before use, the solutions were kept at about 5°C to minimize temperature

changes during solution changes. The buffer consisted of equal parts of MOPS (mor-pholinopropane sulfonic acid, pK_a 7.2), CAPS (cyclohexylaminopropane sulfonic acid, pK_a 10.4), and propionic acid (pK_a 4.9), titrated to the final pH with HCl or NaOH. Since only the sodium currents were being studied, tetraethylammonium bromide (TEA·Br) was used in all bathing solutions to block potassium currents: 120 mM TEA·Br was added 1:10 to the prepared solutions. The measured osmolarity of all solutions varied less than 4%.

The two ends of the nerve fiber were cut in isotonic (120 mM) KCl or in 105 mM KCl plus 15 mM NaCl or in 90 mM KCl plus 30 mM NaCl. When these solutions contained sodium, the node gave large outward sodium currents, indicating that the sodium diffused down the axon to the inside of the node (as tetraethylammonium ion does, Koppenhöfer and Vogel, 1969).

TABLE I
COMPOSITIONS OF SOLUTIONS

	NaCl	KCl	CaCl₂	TMA Cl*	Buffer	pH
	mM	*mM*	*mM*	*mM*	*mM*	
Ringer	115	2.5	2.0	0	6	‡
TMA Ringer	0	2.5	2.0	115	6	‡
⅛ Na Ringer	14	2.5	2.0	101	6	7
High calcium	0	2.5	87	0	6	7

* Tetramethylammonium chloride.
‡ pH of these solutions is buffered to 5, 5.8, or 7 as needed.

RESULTS AND ANALYSIS

Hydrogen Ions Reduce Sodium Currents

Fig. 1 shows the relation between peak sodium currents and voltage at normal pH (pH 7) and at low pH. To obtain each data point, the node is depolarized to the voltage indicated and the peak of the current is measured from records like those in Fig. 2 A. Negative currents represent flow of sodium ions into the axon. Above the sodium equilibrium potential (+43 mV), sodium flux is outward, so currents are positive. Current in potassium channels is negligible at short times, since TEA (tetraethylammonium ion) is present in all solutions.

Lowering the pH to 5.8 reduces the size of sodium currents (I_{Na}) at all voltages by a small amount. Lowering the pH to 5 reduces I_{Na} much more. As Fig. 2 A shows, low pH solutions also slow the kinetics of sodium channel opening and closing (Hille, 1967). All of the changes in sodium currents caused by pH 5 solutions are reversible. The sodium equilibrium potential E_{Na} is not changed appreciably by bathing the nerve in a low pH solution. No change in E_{Na} is expected from thermodynamic considerations, provided that hydrogen ions are not greatly more permeable than sodium through the sodium channel and that hydrogen ions do not alter the channel's selectivity.
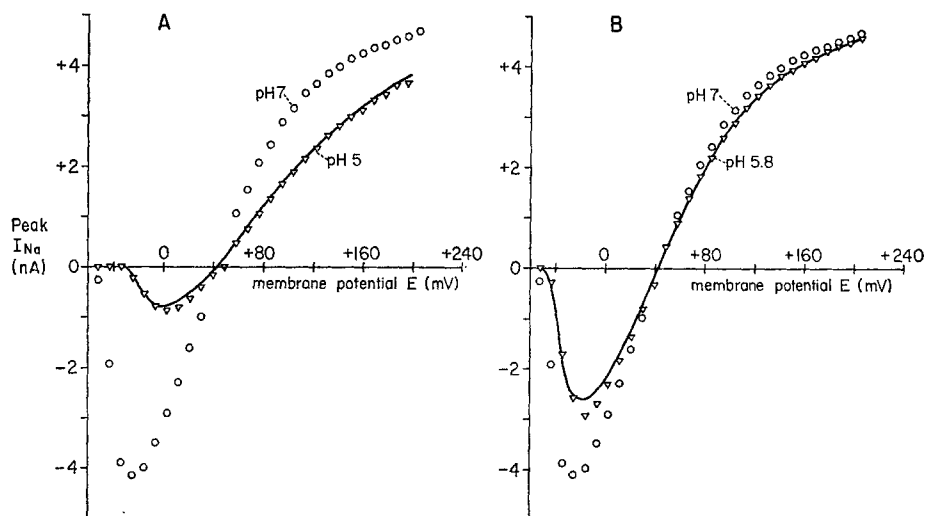
FIGURE 1. Peak sodium currents vs. membrane potential for a frog myelinated nerve fiber in Ringer solutions of normal and low pH. Low pH reduces sodium currents at all membrane potentials, but the depression is partly relieved by raising the membrane potential to large positive potentials. (A), Smooth curve through pH 5 data is derived from the pH 7 curve according to the ionic blockage model with b_{-1}/b_1 = 4.7 × 10^{-6} M, δ = 0.28, and with a voltage shift of +23 mV. (B), Smooth curve through pH 5.8 data is drawn with the same values of the parameters b_{-1}/b_1 and δ as in (A), but with a voltage shift of +6 mV. Node N. (Some of the actual current traces are shown in Fig. 2 A.)

Reduction of Sodium Permeability Depends on Voltage

Fig. 2 B shows values of the peak sodium permeability (P_{Na}) calculated from current measurements like those in Fig. 1. Under normal conditions, P_{Na} can be used as a measure of the number of sodium channels that are open (Dodge and Frankenhaeuser, 1959). For example, in the pH 7 curve in Fig. 2 B, as the voltage becomes more positive P_{Na} increases, indicating that depolarization opens sodium channels. Above +25 mV the number of sodium channels open at the peak of the sodium current is approximately constant, as shown below. Correspondingly, the peak sodium permeability calculated from the currents for pH 7 reaches a plateau. In following analysis it is useful to consider first the changes in P_{Na} caused by pH in this plateau region (at large positive potentials). The changes in P_{Na} at negative potentials are discussed briefly at the end.

At pH 5, sodium permeabilities at all voltages are reduced, compared to the permeabilities at pH 7. Significantly, P_{Na} at pH 5 does not reach a plateau at large positive potentials, but continues to increase as the voltage is increased. Thus while lowering the pH reduces P_{Na}, the amount of reduction becomes less and less as the voltage is raised. Evidently, the block caused by protons is voltage dependent.
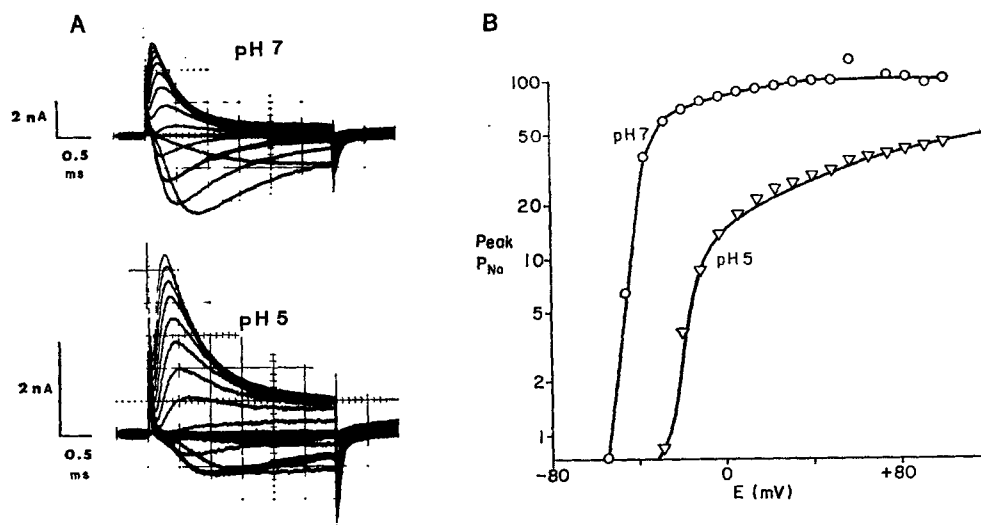
FIGURE 2. Sodium current traces and sodium permeability for a node in Ringer at pH 7 and pH 5. (A), Oscilloscope traces of sodium current vs. time. Note the two different current scales. At pH 5 the currents for large depolarizations are reduced less than those at small depolarizations. The apparent lack of sodium inactivation at pH 5 at large depolarizations may actually be due to a residual potassium current; about 3% of normal potassium current remains in 12 mM TEA solution (Hille, 1967). Such potassium current would not interfere with measurements of I_{Na} at early times. Node N. (B), Peak sodium permeability vs. voltage. At pH 7, sodium permeability increases with depolarization and reaches a plateau. At pH 5, sodium permeability is depressed at all voltages. Above +25 mV the number of sodium channels open at the peak of permeability is nearly constant, but sodium permeability at pH 5 continues to rise with voltage (note logarithmic scale of P_{Na}). Smooth curve for pH 7, arbitrary function. Smooth curve for pH 5 derived from that for pH 7 using the ionic blockage model with $b_{-1}/b_1 = 2.6 \times 10^{-6}$ M, $\delta = 0.26$, and a +23 mV voltage shift. Node B.

A Constant Number of Sodium Channels is Open at Peak of Current

Hydrogen ions could reduce the flow of sodium ions either by changing sodium channel gating (number of sodium channels open) or by reducing the permeability of each channel (the average rate of sodium ion passage). Experiments with quick changes in membrane potential ("instantaneous" clamps) can distinguish between these possibilities. The procedure is as follows: after the usual hyperpolarizing prepulse, the nerve is depolarized to a certain voltage (to be called the "depolarizing voltage"); then at the peak of the sodium current the membrane potential is clamped to -44 mV. The size of the "tail" of inward sodium current is taken as a measure of the number of sodium channels open at the peak of the current (just before the nerve was repolarized to -44 mV). Using this method of tails, Dodge and Frankenhaeuser (1959) found that (at pH 7) the number of sodium channels open at

the peak of the sodium current is approximately constant for depolarizing voltages from 0 to +100 mV.

Using the method of tails, I confirmed the results of Dodge and Frankenhaeuser for nodes at pH 7. An example is shown in the top half of Fig. 3. When the membrane is repolarized after depolarization to +28 mV or to +100 mV, the sodium current tails are nearly identical. Hence, the same
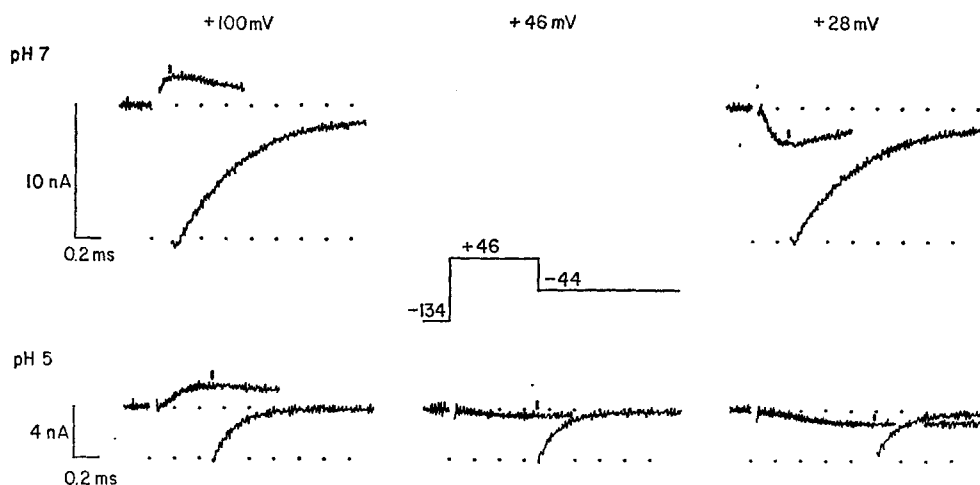

FIGURE 3. Sodium "tails" after a quick change in clamp potential at pH 7 and pH 5. After the membrane potential was clamped to the voltages indicated, the membrane was repolarized to −44 mV at the peak of the sodium current; the time of repolarization is indicated by a vertical mark. Each record shows one long and one short depolarization. The size of the current tails measures the number of sodium channels that were open at the peak of the current. pH 7: At +100 mV and +28 mV the tails are the same. pH 5: At +100 mV and +45 mV the tails are the same; at +28 mV the tail is about 15% smaller. The center record indicates the time-course of the voltage. Leakage current was subtracted electronically, but no capacity current subtraction was made. The sodium equilibrium potential was +58 mV.

number of sodium channels is open at the peak of the current at these two depolarizing voltages. Analysis of the initial size of the sodium tails on repolarization to different voltages has not been possible, perhaps because the voltage clamp response is too slow. However, the method of comparing tails upon repolarization to a constant potential should be valid despite any shortcomings of the clamp.

Similar experiments at pH 5 tested whether a constant number of channels is open at large depolarizing voltages. Fig. 3 shows that at pH 5 the current tails are the same after depolarizing voltages of +46 mV and +100 mV, and are reduced only 15% after a depolarizing voltage of +28 mV. In other words, a nearly constant number of sodium channels is open from +28 to

+100 mV. By contrast, the peak sodium permeability is reduced 47% at +28 mV and 32% at +46 mV, compared to the peak permeability at +100 mV. At pH 5, then, the measured peak sodium permeability changes with voltage, even when a constant number of channels is open.

Other Effects of Low pH and of High Calcium

Hydrogen ions in the bathing solution block both inward and outward flow of sodium ions (Fig. 1). In experiments where all external sodium ions are replaced by tetramethylammonium (TMA) ion, low pH causes voltage-dependent blockage of outward sodium currents. As is shown later the degree of block in these sodium-free solutions is almost identical to that in normal Ringer solution.

Hydrogen ion block is quick. When a pH 7 solution was rapidly replaced by pH 5, the half time for reduction of sodium currents was less than 2 s.

Low pH solutions cause no large changes in the resting potential of frog nodes. Although action potentials are quickly diminished or abolished at pH 5, the nerve is not depolarized. In fact, lowering pH often makes the resting potential up to 15 mV more negative.

In one experiment, the outward sodium currents at low pH increased relative to the currents at pH 7 for potentials above +150 mV. Similarly, at high calcium concentrations, larger outward sodium currents were seen than in the controls, but only at very high potentials; the large currents persisted for some tens of seconds after the solution was changed back to normal calcium. These large currents, which seem anomalous, could result from decreases in long-term inactivation. Lobster and squid axons are known to have long-term inactivation (distinct from the quicker h inactivation of Hodgkin and Huxley), which is seen as a slow increase in sodium currents during a steady hyperpolarization (Narahashi, 1964; Adelman and Palti, 1969). Frog nodes of Ranvier also show such a slow inactivation, dependent on voltage and completed in 1 or 2 min. Hyperpolarizing the node by 30 mV from rest causes the sodium currents slowly to increase about 30%, even though the normal h inactivation is removed before each test pulse by a 40 ms prepulse. Since H^+ and Ca^{++} act in several respects as if the ions were hyperpolarizing the membrane, it is reasonable to propose that these ions may also change the long-term inactivation in the same direction. That is, adding H^+ or Ca^{++} to the medium may change the membrane surface potential, thus decreasing long-term inactivation and thereby increasing sodium currents.

A Theory for Ionic Blockage of Permeability

The results described above indicate that the blockage of sodium permeability by hydrogen ions (as seen at high positive potentials) depends upon the potential across the membrane. Dr. B. Hille suggested to me the following ex-

planation for this voltage-dependent ionic blockage: Hydrogen ions may pass through open sodium channels, but stick inside the channels for a relatively long time. While a hydrogen ion is inside the channel, sodium passage is blocked. If the site where hydrogen ions bind and block is inside the channel, a fraction of the electrical potential drop across the membrane is felt by ions in the site. A positive potential inside the axon would repel hydrogen ions from the binding site and reduce blocking.

The theory of ionic blockage is derived for changes in sodium permeability, but its application is not limited to sodium channels. The theory may apply to block by any "sticky" or slow-moving ion passing through, or partway through, an ionic channel. Similar kinetic models have been proposed by others (e.g., Woodbury, 1971; Baker, 1971; Heckman, Lindemann, and Schnakenberg, 1972) to describe phenomena related to permeability.

ASSUMPTIONS An equation for the fraction of channels blocked by an ion X can be derived by making the following assumptions. The derivation of the general form of the equation is given in the Appendix.

(a) The rates of binding and unbinding of ion X at a site in the channel vary as exponential functions of the membrane potential as in Eyring rate theory.

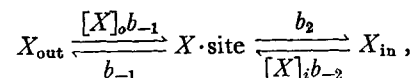(b) When an ion X occupies the blocking site, sodium ions cannot pass through the channel.

(c) Other ions do not interfere with the binding of ion X to the site. Specifically, sodium ions do not compete appreciably.

(d) All channels being considered are open. The model is not concerned with how channels open or close, only with the fraction of open channels that are blocked by ion X.

(e) The current carried by ion X is negligible compared to sodium currents.

(f) The system is in a steady state of blockage; i.e., the time constants for sodium channel opening (0.1–0.3 ms at 5°C) are long compared to the time ion X takes to reach a steady-state concentration in the channel. For hydrogen ion the assumption is almost certainly true, since protonation and deprotonation are very rapid. For acetic acid at 25°C, for example, the rate constant for protonation is 4.5×10^{10} M^{-1} s^{-1} and that for deprotonation is 8×10^{5} s^{-1} (Frost and Pearson, 1961, p. 281). Assuming a Q_{10} of 2.5 for both processes, the time constants for protonation and deprotonation at 5°C and pH 5 are about 11 and 8 μs.

Then in the general form of the model the blocking ion X can reach the blocking site from either inside or outside the axon. At zero potential across the membrane, the rates of entering and leaving the site are as shown in this schema:

$$X_{\text{out}} \underset{b_{-1}}{\overset{[X]_o b_{-1}}{\rightleftarrows}} X \cdot \text{site} \underset{[X]_i b_{-2}}{\overset{b_2}{\rightleftarrows}} X_{\text{in}} ,$$

where the b_i are the voltage-independent components of the rate constants; $[X]_o$ and $[X]_i$ are the concentrations of the blocking ion outside and inside the axon. For membrane potentials other than zero the b_i must be multiplied by exponential functions of voltage to obtain the rate constants, as described in the Appendix.

Application of the Ionic Blockage Model to Data

METHOD OF DATA ANALYSIS By the assumptions of the model, sodium ions pass through an open sodium channel only when the channel is not occupied by a blocking ion. Hence, the sodium current should be proportional to the fraction of channels not blocked. At a given voltage, for two different concentrations of blocking ions, the difference in the amount of sodium current measured should be due to different fractions of the sodium channels being blocked, provided that the number of channels open is constant. Then from Eq. (7 *a*) in the Appendix, the ratio of the sodium current at pH 5 to the current at pH 7 is

$$\frac{I_{pH\,5}}{I_{pH\,7}} = \frac{p_{pH\,5}}{p_{pH\,7}} = \frac{10^{-7} + K(E)}{10^{-5} + K(E)}, \tag{1}$$

where

$$K(E) = [X]_i \frac{b_{-2}}{b_1} \exp\left(\frac{zFE}{2RT}\right) + \frac{b_{-1}}{b_1} \exp\left(\frac{z\,\delta\,FE}{RT}\right)$$

$$+ \frac{b_2}{b_1} \exp\left(\frac{(2\,\delta - 1)zFE}{2RT}\right). \tag{2}$$

Here $I_{pH\,5}$ is the sodium current at a particular voltage in a bathing solution of pH 5; $I_{pH\,7}$ is the sodium current at the same voltage at pH 7. The fractions of sodium channels not blocked by hydrogen ions at that same voltage at each pH are $p_{pH\,5}$ and $p_{pH\,7}$. The b_i are explained above. The fraction of the membrane potential acting at the site is δ; z is the valence of the blocking ion; and E, F, R, and T are the electrical potential across the membrane, the Faraday, the gas constant, and the absolute temperature, respectively.

It is convenient to use the term $K(E)$ for data analysis, because $K(E)$ can be calculated from measured sodium currents by Eq. (1), and because $K(E)$ contains all the parameters of the model. Since the model does not take explicit account of possible changes in gating of channels, Eq. (1) applies strictly only at high positive potentials, where a constant number of sodium channels is open.

To evaluate the relative importance of the three independent parameters of the general model, I used Eq. (2) to calculate expected $K(E)$ values at six different voltages for hundreds of different combinations of values of b_{-1}/b_1, b_2/b_1, and δ. Each parameter was varied over all of its possible range. The

value of b_{-2}/b_1 was obtained from Eq. 8 a. The expected values of $K(E)$ were compared to the values computed from the currents in a nerve at pH 5 and pH 7 via Eq. (1), and the variance (the sum of the squared differences divided by six) was computed. The variance was small only for the cases in which b_2/b_1 and b_{-2}/b_1 were close to or equal to zero. That is, the model will fit the data only when the rates of H^+ ions moving from the blocking site to the axoplasm and back are made quite small or zero. Therefore, it is possible to use a simpler model, in which these rates are assumed to be zero, and H^+ ions block only from the external medium.

The equation for sodium current when b_2 and b_{-2} are zero becomes, from Eq. (7 a)

$$I_{Na} \alpha p = \frac{K(E)}{[X]_o + K(E)},$$ (3)

where

$$K(E) = \frac{b_{-1}}{b_1} \exp\left(\frac{z \delta FE}{RT}\right),$$ (4)

or

$$I_{Na} \alpha p = \frac{b_{-1}/b_1}{[X]_o \exp\left(\frac{-z \delta FE}{RT}\right) + b_{-1}/b_1}.$$ (5)

As before, p is the fraction of channels not blocked by X ions (in this case, hydrogen ions). The two parameters are b_{-1}/b_1, the dissociation constant of X ion from the channel site [or $K(E)$ measured at zero applied potential], and δ, the fraction of the membrane potential acting on an ion in the site.

The simplified Eq. (3) says that I_{Na} should titrate away as the external pH is lowered. If measured at a constant voltage the titration curve should have the same shape as the titration of an ordinary acid. Indeed previous work (Hille, 1968; Drouin and The, 1969) has already shown such a simple titration behavior. The new result in Eq. (3) or (5) is that the apparent dissociation constant of the titrating site should increase as the internal potential is made more positive. Specifically, the values of $K(E)$ calculated from the ratios of sodium currents at pH 5 and pH 7 should depend exponentially upon voltage, Eq. (4).

BLOCKAGE DEPENDS ON POTENTIAL AS PREDICTED BY THEORY   A convenient measure of the depression of sodium currents by H^+ ion is the ratio of the sodium current at low pH to the current at pH 7. Taking the ratio of the sodium currents at each voltage eliminates the nonlinearities of the current-voltage relation and leaves the effects due to blocking. Fig. 4 A shows
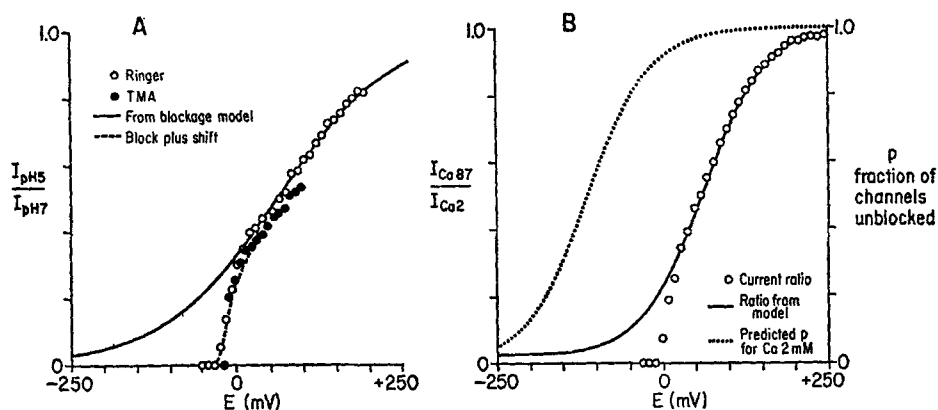
FIGURE 4. Voltage dependence of the H^+ and Ca^{++} blockage of sodium currents. (A), Ratio of sodium currents at low pH to currents at normal pH as a function of voltage. O, Data from a node bathed in Ringer (Node N). Smooth curve is from Eq. (1) and (4) for ionic blockage with $b_{-1}/b_1 = 4.7 \times 10^{-6}$ M, $\delta = 0.28$ to fit Node N. Dashed curve is calculated by taking both blocking and voltage shift into account, by shifting the pH 7 P_{Na} curve $+23$ mV along the voltage axis. ●, Data from a node bathed in a sodium-free solution (with TMA ion, Node K); this node had slightly different parameters, so the points do not lie on the same smooth curve. (B), Ratios of outward sodium currents in 87 mM Ca^{++} to currents in TMA solution. Circles are measured current ratios; the currents in high calcium have been divided by 1.3 to take into account a decrease in long-term inactivation. Smooth curve is predicted from Eq. (1) and (4) with $b_{-1}/b_1 = 23$ mM and $\delta = 0.26$. Deviation of data from curve below $+25$ mV is probably due to voltage shifts as seen in the dashed line in part (A) of the figure. Dotted line, predicted fraction of channels unblocked by calcium in ordinary Ringer solution with 2 mM calcium, calculated from Eq. (3) and (4) with b_{-1}/b_1 and δ the same as for the solid curve. Blockage of sodium channels by calcium ions in Ringer is negligible at voltages more depolarized than the resting potential.

the sodium current ratio for pH 5 compared to pH 7, as a function of voltage. As already mentioned, the steady rise of the ratio with membrane potential indicates that sodium channels are less blocked at large positive potentials.

The apparent dissociation constant of the blocking site, $K(E)$, can be calculated from the sodium current ratio using Eq. (1) or Eq. (3). Values of the logarithm of $K(E)$ plotted vs. voltage fall close to a straight line, Fig. 5, so $K(E)$ apparently obeys the theoretical relation of Eq. (4). From such plots the parameters b_{-1}/b_1, the dissociation constant at zero applied potential, and δ, the fraction of membrane potential acting at the site, are obtained. Values from several nodes are summarized in Table II. The average b_{-1}/b_1, 3.9×10^{-6} M, corresponds to an acid site with a pK_a of 5.4. The average value of δ, 0.26, means that the site is about one-quarter of the way across the membrane's potential from the outside (but not necessarily one-quarter of the distance across the membrane, if the electrical field is not constant).
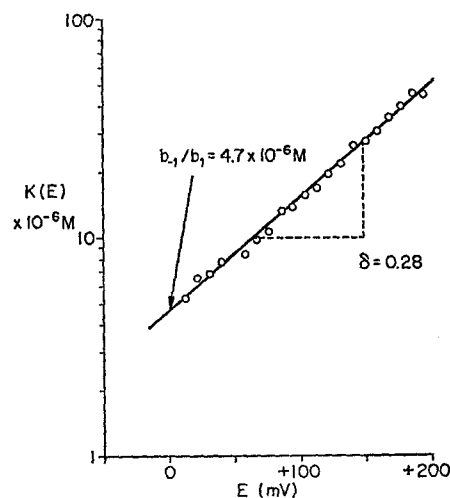
FIGURE 5. Dissociation constant for H^+ blockage as a function of voltage. The circles, values of $K(E)$ are calculated from the sodium currents at pH 7 and pH 5 by Eq. (1). The straight line was fitted by eye to the points above $+20$ mV. The model, in Eq. (4), predicts that $K(E) = b_{-1}/b_1 \exp (z\delta FE/RT)$. Since the slope of the line is 85 mV per e-fold change in $K(E)$, and since $zF/RT = 0.0417$ mV^{-1}, δ is 0.28. The value of b_{-1}/b_1 is found from the intercept of the line where $E = 0$. Here $b_{-1}/b_1 = 4.7 \times 10^{-6}$ M. Node N in Ringer solutions.

TABLE II

VALUES OF THE PARAMETERS FOR H^+ BLOCKAGE OF
SODIUM CHANNELS

Node	Mean value* of δ	Mean value* of b_{-1}/b_1
		μM
B	0.298	2.2
G	0.197	1.5
K‡	0.288	4.5
L‡	0.267	7.0
M	0.240	2.3
N	0.231	6.2
Mean of all nodes (± SD)	0.26 (±0.04)	3.9 (±2.3)

* The values for the parameters of each node are the mean of two or more determinations from graphs such as Fig. 5.
‡ Nodes K and L were bathed in TMA solutions with no sodium present.

Two of the nodes in Table II were bathed in TMA (tetramethylammonium ion) solution, with no sodium present; some data from one of these are in Fig. 4 A. The parameters calculated from these nodes are in the same range as those from nodes in Ringer solution. Sodium ions competing for the site would increase the apparent value of b_{-1}/b_1. However, the values of b_{-1}/b_1

are if anything larger in the absence of sodium, so there is no evidence of competition between sodium and hydrogen ions.

P_{Na}/p AS A MEASURE OF NUMBER OF OPEN CHANNELS   In normal Ringer solution, P_{Na} is a good measure of the number of sodium channels whose "gates" are open. But when hydrogen ions are added to the solution, some of the open channels are blocked, so that only the fraction p of the channels is left to conduct sodium ions. Since p can now be calculated from the theory, it should be possible to calculate the number of sodium channels with open gates by dividing the measured P_{Na} by the value of p (which depends on the voltage and pH).

Fig. 6 shows the results of thus correcting P_{Na} for H$^+$ ion blockage. The corrected P_{Na}/p curve for pH 5 has approximately the same shape as the P_{Na} curve at pH 7, although the parent P_{Na} curve at pH 5 had quite a different shape. The P_{Na}/p curve at pH 5 is simply shifted along the voltage axis +23 mV relative to the pH 7 P_{Na} curve. (At pH 7, the correction for blockage is negligible, so P_{Na} and P_{Na}/p are identical.) The identity of shape of these curves suggests that the effects of hydrogen ions on sodium currents arise from two quite separate actions: (a) the voltage-dependent blocking described by the proposed model, and (b) changes in the responses of m and h "gates."
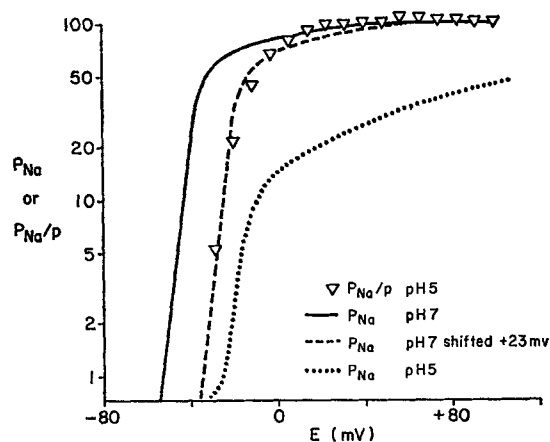

FIGURE 6.   Sodium permeability and permeability corrected for H$^+$ blockage, for a node at pH 7 and pH 5. Solid curve and dotted curve, sodium permeability at pH 7 and pH 5, from Fig. 2 B. ∇, Sodium permeability at pH 5 corrected for blockage by dividing by p, the fraction of channels not blocked. Values of p are from Eqs. (3) and (4) with $\delta = 0.26$ and $b_{-1}/b_1 = 2.6 \times 10^{-6}$ M. The points for P_{Na}/p fall fairly close to the P_{Na} curve from pH 7, when that curve is shifted 23 mV along the voltage axis. These curves illustrate the separation of blockage from voltage shift. Node B.

PREDICTION OF CURRENT-VOLTAGE CURVES AT pH 5.8, pH 5, AND pH 4.4
Current-voltage curves at pH 5 and pH 5.8 were predicted from the current-
voltage curve at pH 7, as a test of the ionic blockage model. Three param-
eters were used: the two parameters of the ionic blockage model (b_{-1}/b_1 and
δ), determined from the data for pH 5 and pH 7 at large positive potentials;
and the voltage shift, determined from plots like Fig. 6. The predictions were
made from the calculated curve of P_{Na} vs. voltage for pH 7. First the P_{Na}
curve was shifted along the voltage axis ($+23$ mV for pH 5 and $+6$ mV for
pH 5.8) to take into account the shift in voltage dependence of m and h gates.
The portion of the P_{Na} curve above E_{Na} was not shifted. Then the sodium
current was calculated for each P_{Na} via the Goldman equation. The fraction
of channels unblocked was calculated from Eqs. (3) and (4) using the same
values of the parameters for pH 5 and pH 5.8; the previously calculated cur-
rent was multiplied by the fraction of channels unblocked. The predictions,
shown as solid curves in Fig. 1 A and 1 B, fit the data reasonably well.

In addition to pH 5.8, the sodium currents at pH 4.4 can be predicted,
if long-term inactivation is taken into account. In one experiment where
pH was lowered both to 5 and to 4.4, it was necessary to assume that long-
term inactivation decreased by 20% at pH 5 and 30% at pH 4.4. When
these corrections are made, the model adequately predicts currents at pH 5
and at pH 4.4 from pH 7 data, by the process described above.

APPLICATION OF THE MODEL TO Ca^{++} DATA   In a few experiments all the
sodium ion in the medium was replaced by TMA ion (with 2 mM calcium
present) or by calcium. The ratios of outward sodium currents in high cal-
cium to outward currents in TMA solutions, shown in Fig. 4 B, closely re-
semble the current ratios for pH 5 and pH 7 in their general dependence on
voltage. The smooth curve through the calcium data was drawn according
to Eqs. (3) and (4), with $\delta = 0.26$, $b_{-1}/b_1 = 23$ mM, and $z = 2$. From the
good fit of the model to the calcium data, it appears that calcium ions at high
concentrations block sodium channels just as H$^+$ ions do. The block is com-
pletely relieved by raising the membrane potential to $+250$ mV. The devia-
tion of the data points from the smooth curve below $+20$ mV is probably
due to voltage shifts as seen for H$^+$ data in the dashed line in Fig. 4 A. Note
that for this analysis of the calcium data it was assumed that long-term in-
activation was decreased 30% in high calcium, and sodium currents were
scaled accordingly.

DISCUSSION

Dual Effects of Hydrogen Ion on I_{Na}

This paper presents evidence that hydrogen ion affects sodium currents both
by blocking sodium passage, as described by the ionic blockage model, and
by shifting the responses of the sodium channel "gates" to voltage. Purely

blocking effects are best seen at positive membrane potentials above $+25$ mV. In this voltage range a constant number of sodium channels is open (as shown in Fig. 3), so the steady increase of P_{Na} with voltage must be ascribed to a decrease in the number of channels blocked. On the other hand, the voltage shifts caused by low pH affect sodium currents most in the range from -50 to 0 mV. The shifts are in the direction to be expected if hydrogen ions bind to the outer surface of the membrane and cause a change in surface potential, thus influencing the responses of the channel gates (Hille, 1968).

Both the shifts caused by H^+ ion and a decrease in sodium permeability have previously been reported, as summarized below. The new feature of this study is the quantitative test of a model for voltage-dependent hydrogen ion blockage of sodium permeability.

PREVIOUS DATA ON NODES My results agree with other voltage clamp studies of the effects of pH on sodium currents. Hille (1968) and Drouin and The (1969) reported that the sodium permeability of frog nodes decreases with decreasing pH, with a pK_a of about 5.2. Neither of these previous reports mentioned the voltage dependence of H^+ blockage at positive voltages. For an average node, I found an apparent pK_a of 5.4 at 0 mV and 5.2 at $+45$ mV. Besides the decrease in permeability, Hille reported shifts in the P_{Na} curve caused by changing pH.

My analysis differs from that of Drouin and The (1969). They used the ratio of sodium currents at low and normal pH as a measure of the effects of hydrogen ions, as that ratio is used here, but Drouin and The were looking mainly at currents in the voltage range -50 to $+20$ mV (absolute scale). Hence they were mainly observing changes that Hille (1968) and I interpret as shifts in the response of sodium channel gates to voltage, although they interpret their data differently. The model of Drouin and The predicts a constant sodium current ratio above about $+30$ mV, i.e. a voltage-independent pK_a, but in fact the pK_a depends on voltage.

H^+ EFFECTS ON SQUID AXONS From the few voltage clamp experiments that have been published, it appears that H^+ ions block sodium channels in squid axons, as in frog nodes, but the block may develop more slowly. Ehrenstein and Fishman (1971) showed current-voltage curves in which decreasing external pH decreased I_{Na}, but the curves are not complete enough to tell whether their shape altered with pH. If the block depends on voltage in squid axons as in nodes, the normally linear part of the current-voltage curve should become concave upward at low pH, since blockage would be more complete at the negative voltages. Stillman, Gilbert, and Lipicky (1971, and Gilbert, Stillman, and Lipicky, 1972) report that the "maximum sodium current" measured in a ramp clamp decreases with decreasing external pH. However, it is difficult to make a direct comparison between their data, obtained with

a ramp clamp, and peak sodium current data from a conventional voltage clamp like that used in this study. Comparison is especially difficult in studies of pH, because time constants for sodium currents vary with pH (Hille, 1968), but the voltage ramp used by Gilbert, Stillman, and Lipicky was advanced at the same rate (68 mV/ms) regardless of pH.

The slow time-course of changes in the sodium currents of squid axons after changes in external pH contrasts with the speedy changes in frog nodes. Both Bicher and Ohki (1972) and Stillman, Gilbert, and Lipicky (1971) noted that the changes took 5 min or more to develop. It may be that the Schwann cell surrounding the squid axon buffers so effectively that the pH near the working surface of the axon changes only slowly. If this is the explanation for the slow changes in I_{Na} in squid axons, using higher concentrations of buffer should hasten changes.

INTERNAL pH   It is possible that lowering external pH leads to a decrease in sodium permeability by first causing internal pH to drop. Bicher and Ohki (1972) obtained evidence of a decrease in the pH inside squid axons, as measured by a pH microelectrode. They found that after external pH was lowered to 5, the internal pH decreased from 7.0 to 6.3 over a period of 6 or 7 min. A reduction of the resting potential and changes in the action potential followed the drop in internal pH. Although the pH inside the frog node of Ranvier is unknown and may vary, it is unlikely that internal pH mediates the decrease in permeability, from the following argument. In the frog node the changes in I_{Na} after lowering external pH are complete in a few seconds. To change the internal pH of the node so rapidly would require an appreciable current of H^+ ions. If the axoplasm has 10 mM buffering capacity and the volume in 50 μm length of axon (diameter 10 μm) must be changed by 0.5 pH unit in 2 s, then a 1 nA inward current would be required to carry sufficient hydrogen ions to achieve the pH change. Such a flux of H^+ ions inward would depolarize the resting membrane by 40 mV, but no such depolarization is seen.

On the other hand, internal pH directly affects sodium currents in the squid axon. Ehrenstein and Fishman (1971) changed the pH inside squid axons by perfusing internally with buffers. They found that sodium currents were more sensitive to changes in internal than external pH. The large drop in I_{Na} at internal pH 6.5 is not explained by the ionic blockage model if the blockage parameters of squid are like those of the frog node (where H^+ ions apparently enter the channel much more easily from the outside than from the inside). Of course, nothing in the model precludes other mechanisms from shutting down the sodium channel in response to low internal pH. Since the internal pH of the frog node is not readily controlled, further experiments with perfused squid axons, varying internal and external pH independently,

should clarify the status of the ionic blockage model with respect to the questions raised by Bicher and Ohki and by Ehrenstein and Fishman.

Justification of Assumptions of the Model

The ionic blockage model, which is proposed to account for the blockage of sodium currents by hydrogen ions, is a very simple mechanism, leading to simple equations. Are the assumptions involved tenable?

(a) Hydrogen ions enter the sodium channel. A priori, this is likely, since hydrogen ions are small and positively charged.

(b) When hydrogen ion is in the blocking site, no sodium ions can pass through the channel. The block need not be total; the data are not precise enough to say whether the presence of a hydrogen ion might merely slow sodium passage by a factor of 10 or more.

(c) Other ions do not compete with H^+ for the site. External sodium ions probably do not compete since bathing solutions with TMA in place of sodium yielded similar values of the H^+ blocking parameters (Table II). There are no data on the effects on H^+ blockage of changing calcium or potassium ion concentrations.

(d) Hydrogen ions do not pass through the channel. The best fit of the general model suggested that hydrogen ions pass from site to the axoplasm $\frac{1}{100}$ as easily as from the site to the bathing medium at zero applied potential. This fraction is small enough to be ignored in using the model, but it should not be inferred that hydrogen ions are absolutely excluded from passage.

(e) Hydrogen ions contribute negligibly to the measured current. Even at pH 4 the concentration of hydrogen ions is only $\frac{1}{1000}$ that of sodium ions, so hydrogen ions are not expected to enter channels at a high rate. Once inside the channel, hydrogen ions find it about a hundred times easier to exit back to the bathing medium than to go on to the axoplasm (according to the best fit of the general model for blockage). Hence, the rate of H^+ ions going through the sodium channel is small.

(f) Blockage occurs so quickly that it is seen in steady state at the peak of the sodium current. The best evidence for a very rapid equilibration of the block is seen in Fig. 3 in the sodium tails at pH 5. At the depolarizing potentials of +46 and +100 mV, the sodium channels were, respectively, 52 and 27% blocked, yet the tails have identical time-courses, after the first 20 μs in which the trace is too faint to read. Evidently, the new steady state of block is achieved in 20 μs or less.

(g) A tacit assumption in the application of the model is that changes in surface potential of the axon have no effect on blocking. For instance, at pH 5 the surface potential of the outside of the axon is apparently about 20 mV more positive than at pH 7, from the shifts of m and h parameters. One effect of a more positive surface potential would be to lower the local concentration

of H^+ at the blocking site in accordance with the Boltzmann distribution, or in other words to shift the relation of $K(E)$ to voltage shown in Fig. 5. Such a shift of 20 mV or less at the site causes an error in the determination of the parameter b_{-1}/b_1 that is small compared to the standard deviation of the parameter. However, changes in surface potential are capable of causing systematic errors in the calculation of the dissociation constant of the site.

The Sodium Channel

In their elegant analysis of ionic currents, Hodgkin and Huxley (1952) made the first clear separation between gating of sodium channels (described by m and h parameters) and permeability (for which Hodgkin and Huxley used conductance). Since then it has been found that some ions (e.g., Ca^{++}, Ni^{++}, Frankenhaeuser and Hodgkin, 1957; Hille, 1968) can shift the gates' response to voltage, while having little or no effect on the permeability of each channel; i.e., the shape of the P_{Na} vs. voltage curve remains constant. Other ions (ammonium, Li^+, aminoguanidine) can pass through the sodium channels with various rates or permeabilities, while apparently not changing the response of the channel gates to voltage (Hille, 1971, 1972). From these data it appears that the sodium channel has voltage-sensitive gates that open to reveal a rather rigid, voltage-insensitive pore or filter, through which sodium ions must pass.

Numerous investigators have suggested that opening of sodium channel (m) gates might be accomplished by the movement of calcium ions out of blocking positions in sodium channels (e.g., Goldman, 1964; Fishman, Khodorov, and Volkenstein, 1971). In 1957 Frankenhaeuser and Hodgkin pointed out that such calcium gating models cannot explain quantitatively the voltage shifts caused by calcium. For additional criticisms of calcium models see Hille (1972) and Woodhull (1972). The data on calcium presented here indicate that, in addition to causing shifts, calcium ions may block open sodium channels. However, the characteristics of this calcium block are all wrong for calcium to serve as the sodium channel gate: (a) Calcium at physiological concentrations (2 mM in frog) does not block 50% of the channels until the node is hyperpolarized to −100 mV, whereas almost all sodium channels are closed for voltages more negative than −80 mV. (b) Most important, the steepest voltage dependence of calcium blockage is 13 times less steep than the voltage dependence of the increase of P_{Na} with depolarization. The evidence for voltage-dependent calcium block is in better agreement with the idea that calcium ions can pass slowly through open sodium channels (Baker, Hodgkin, and Ridgway, 1971) than with the concept of calcium ions as sodium channel gates.

Like calcium ions, hydrogen ions change both the gating and the permeability of sodium channels, but this paper has shown that the two effects can

be separated. The changes in permeability can be explained as temporary blockages of the open sodium channel, caused by H^+ ions sticking at a site part way through the channel. The pK_a of 5.4 of the blocking site (at 0 mV) suggests that the site is the carboxylic acid group in the selectivity filter described by Hille (1971, 1972). The voltage dependence of both H^+ and Ca^{++} blocking places this acid group, and the filter, about one-quarter of the way into the membrane from the outside. When the H^+ blockage is corrected for, the changes in gating caused by H^+ can be seen as simple shifts in the responses of the sodium channel gates to voltage. It is likely that protons cause these shifts by changing the surface potential of the axon membrane.

APPENDIX

An equation describing the probability of blockage of a channel by an ion can readily be derived from the assumptions given in the text. Assume that there is one ion-binding site inside the channel. An ion X (for example, H^+) can reach the site from either inside or outside the axon.

$$X_{\text{OUT}} \underset{k_{-1}}{\overset{k_1}{\rightleftharpoons}} X \cdot \text{SITE} \underset{k_{-2}}{\overset{k_2}{\rightleftharpoons}} X_{\text{IN}}.$$
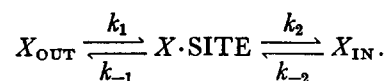
Here the k_i are the rate constants (in seconds^{-1}) for ion movement in the directions specified; k_1 and k_{-2} are pseudo first-order rate constants, as they include the factors for outside and inside concentrations of ion X.

In the steady state, the probability (p) that a site is *not* occupied is constant, and is (from chemical kinetics)

$$p = \frac{k_{-1} + k_2}{k_1 + k_2 + k_{-1} + k_{-2}}. \tag{1 a}$$

That is, the probability that a channel site is not occupied by a blocking ion is the ratio of the sum of rates for leaving the site to the sum of all rates for entering and leaving.

Now assume that ion X affects the measured sodium currents only by blocking sodium ion passage, and not by carrying current. Sodium current is then proportional to the fraction of channels not blocked. Hence Eq. (1 a) can describe blockage of sodium currents, if the equation is put into a form in which the parameters may be determined experimentally. From Eyring rate theory (Eyring and Eyring, 1963) as it has been applied to movement of ions in channels (Woodbury, 1971; Baker, 1971; Heckman, Lindemann, and Schnakenberg, 1972), the blocking site in the channel is an energy minimum in the movement of ion X through the membrane (Fig. 7 A). To pass from the bathing solution into the site, ion X must go over an energy barrier of height U_1. This barrier might represent the shedding of some waters of hydration. Each rate of ion movement, k_i, depends upon the corresponding energy barrier, U_i. When a voltage (E) is applied, a fraction δ of the voltage is assumed to be felt by the ion in the site. The corresponding electrical potential energy adds to each energy

barrier. Then the expressions for the rate constants are

$$k_1 = [X]_o \, a_1 \exp\left(\frac{-U_1}{RT} - \frac{z \, \delta \, FE}{2RT}\right), \tag{2 a}$$

$$k_{-1} = a_{-1} \exp\left(\frac{-U_{-1}}{RT} + \frac{z \, \delta \, FE}{2RT}\right), \tag{3 a}$$

$$k_2 = a_2 \exp\left(\frac{-U_2}{RT} - \frac{z(1 - \delta)FE}{2RT}\right), \tag{4 a}$$

$$k_{-2} = [X]_i \, a_{-2} \exp\left(\frac{-U_{-2}}{RT} + \frac{z(1 - \delta)FE}{2RT}\right), \tag{5 a}$$

where $[X]_o$ and $[X]_i$ are the concentrations of the blocking ion X outside and inside the axon. (These are the bulk concentrations; if the concentrations at the membrane are different from those in bulk, the proportionality constants are included in constants a_1 and a_{-2}.) The U_i are voltage-independent components of the activation energies, the a_i are constants, and z is the number of electronic charges on ion X. R is the gas constant, T the absolute temperature, F Faraday's constant, and E the membrane potential. Both the a_i and the U_i are unknown constants, so they may be combined. Let

$$b_i = a_i \exp\left(\frac{-U_i}{RT}\right). \tag{6 a}$$

With Eq. (2 a) through (6 a) substituted into equation (1 a), the general expression for the probability that a channel is not blocked becomes:

$$p = \frac{\dfrac{b_{-1}}{b_1} \exp\left(\dfrac{z \, \delta \, FE}{RT}\right) + \dfrac{b_2}{b_1} \exp\left(\dfrac{(2\delta - 1)zFE}{2RT}\right)}{[X]_o + [X]_i \dfrac{b_{-2}}{b_1} \exp\left(\dfrac{zFE}{2RT}\right) + \dfrac{b_{-1}}{b_1} \exp\left(\dfrac{z \, \delta \, FE}{RT}\right) + \dfrac{b_2}{b_1} \exp\left(\dfrac{(2\delta - 1)zFE}{2RT}\right)}. \tag{7 a}$$

Eq. (7 a) is a general expression describing blocking of a membrane pore by an ion, when the ion can enter the pore from either side of the membrane. This equation might find application in any situation in which there is one major energy minimum for a blocking ion at some location inside a channel.

Not all of the constants b_i are independent. At zero applied voltage and with equal concentrations of X on both sides of the membrane, the net transport must be zero, whence this restriction may be derived:

$$\frac{b_{-2}}{b_2} = \frac{b_1}{b_{-1}}. \tag{8 a}$$

This expression may be used to eliminate any one of the b_i from Eq. (7 a).

PREDICTIONS OF THE GENERAL THEORY   The general model for ionic blockage of channels, Eq. (7 a), has only three independent parameters: b_{-1}/b_1, the rate constant for blocking ions' returning to the bathing solution relative to their rate of

entering the blocking site from the solution; b_{-2}/b_1, the relative rate constant for ions' entering the site from the axoplasm; and δ, the fraction of membrane potential acting at the site. Fig. 7 shows how the fraction of channels not blocked by a positive ion X depends upon membrane potential for some choices of parameter values. Parameter δ determines how steeply the degree of block depends on voltage (Fig. 7 B). Changing the relative heights of the energy barriers to ion movement, or the relative values of the b_i, has dramatic effects on the voltage-dependence of the blocking, as seen in Fig. 7 C. If a positive ion blocks mainly by entering from the outside (b_{-2} small), raising the membrane potential relieves the block. If the block is mostly from the axoplasm
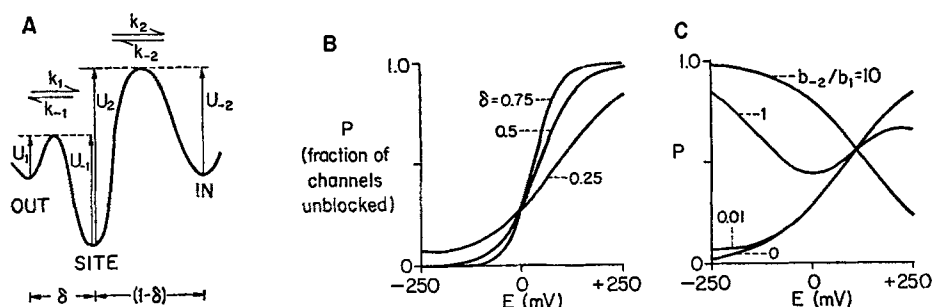

FIGURE 7. Some features of the general model for ionic blockage of channels. (A), A sketch of the energy profile of the channel from the point of view of the blocking ion, showing the heights of energy barriers U_i and the rate constants k_i. An applied voltage would add fractionally to each energy; the fraction δ of the voltage would be felt at the site. (B) and (C), The effects of changing two of the model's parameters on the voltage dependence of blocking. The fraction of channels not blocked by X is called p. Except where noted, the parameters have the following values, which were chosen to approximate those of a frog node bathed in pH 5 solution: $[X]_o = 10^{-5}\ M$, $[X]_i = 10^{-7}\ M$, $\delta = 0.25$, $b_{-1}/b_1 = 4 \times 10^{-6}\ M$, $b_{-2}/b_1 = 0.01$, and consequently $b_2/b_1 = 4 \times 10^{-8}\ M$ from Eq. (8 a).

(b_{-2} large), raising potential increases blocking by driving ions into the blocking position. At a fixed membrane potential Eq. (7 a) simply predicts that increasing either the external concentration of blocking ions, $[X]_o$, or the internal concentration, $[X]_i$, will decrease the fraction of channels unblocked.

REFERENCES

ADELMAN, W. J., and Y. PALTI. 1969. The effects of external potassium and long duration voltage conditioning on the amplitude of sodium currents in the giant axon of the squid, *Loligo pealei*. *J. Gen. Physiol.* 54:589.

ARMSTRONG, C. M., and B. HILLE. 1972. The inner quaternary ammonium ion receptor in potassium channels of the node of Ranvier. *J. Gen. Physiol.* 59:388.

BAKER, M. 1971. Ion transport through nerve membranes. Doctoral dissertation. University of Washington, Seattle. University Microfilms, Inc., Ann Arbor, Mich.

BAKER, P. F., A. L. HODGKIN, and E. B. RIDGWAY. 1971. Depolarization and calcium entry in squid giant axons. *J. Physiol. (Lond.)* 218:709.

BICHER, H. I., and S. OHKI. 1972. Intracellular pH electrode experiments on the giant squid axon. *Biochim. Biophys. Acta.* 255:900.

DODGE, F. A., and B. FRANKENHAEUSER. 1958. Membrane currents in isolated frog nerve fibre under voltage clamp conditions. *J. Physiol. (Lond.)* 143:76.

DODGE, F. A., and B. FRANKENHAEUSER. 1959. Sodium currents in the myelinated nerve fibre of *Xenopus laevis* investigated with the voltage clamp technique. *J. Physiol. (Lond.)* 148:188.

DROUIN, H., and R. THE. 1969. The effect of reducing extracellular pH on the membrane currents of the Ranvier node. *Pfluegers Arch. Eur. J. Physiol.* 313:80.

EHRENSTEIN, G., and H. M. FISHMAN. 1971. Evidence against hydrogen-calcium competition model for activation of electrically excitable membranes. *Nat. New Biol.* 233:16.

EYRING, H., and E. M. EYRING. 1963. Modern Chemical Kinetics. Van Nostrand Reinhold Company, New York.

FISHMAN, S. N., B. I. KHODOROV, and M. V. VOLKENSTEIN. 1971. Molecular mechanisms of membrane ionic permeability changes. *Biochim. Biophys. Acta.* 225:1.

FRANKENHAEUSER, B., and A. L. HODGKIN. 1957. The action of calcium on the electrical properties of squid axons. *J. Physiol. (Lond.)* 137:218.

FROST, A. A., and R. G. PEARSON. 1961. Kinetics and Mechanism. John Wiley & Sons, Inc., New York.

GILBERT, D. L., I. M. STILLMAN, and R. J. LIPICKY. 1972. Effect of external pH on the sodium currents in the squid giant axon. Abstracts of International Union for Pure and Applied Biophysics, Moscow, August, 1972. 227.

GOLDMAN, D. E. 1943. Potential, impedance, and rectification in membranes. *J. Gen. Physiol.* 27:37.

GOLDMAN, D. E. 1964. A molecular structural basis for the excitation properties of axons. *Biophys. J.* 4:167.

HECKMANN, K., B. LINDEMANN, and J. SCHNAKENBERG. 1972. Current-voltage curves of porous membranes in the presence of pore-blocking ions. I. Narrow pores containing no more than one moving ion. *Biophys. J.* 12:683.

HILLE, B. 1967. The selective inhibition of delayed potassium currents in nerve by tetraethylammonium ion. *J. Gen. Physiol.* 50:1287.

HILLE, B. 1968. Charges and potentials at the nerve surface. Divalent ions and pH. *J. Gen. Physiol.* 51:221.

HILLE, B. 1971. The permeability of the sodium channel to organic cations in myelinated nerve. *J. Gen. Physiol.* 58:599.

HILLE, B. 1972. The permeability of the sodium channel to metal cations in myelinated nerve. *J. Gen. Physiol.* 59:637.

HODGKIN, A. L., and B. KATZ. 1949. The effect of sodium ions on the electrical activity of the giant axon of the squid. *J. Physiol. (Lond.)* 108:37.

HODGKIN, A. L., and A. F. HUXLEY. 1952. A quantitative description of membrane current and its application to conduction and excitation in nerve. *J. Physiol. (Lond.)* 117:500.

KOPPENHÖFER, E., and W. VOGEL. 1969. Effects of tetrodotoxin and tetraethylammonium chloride on the inside of the nodal membrane of *Xenopus laevis*. *Pfluegers Arch. Eur. J. Physiol.* 313:361.

NARAHASHI, T. 1964. Restoration of action potential by anodal polarization in lobster giant axons. *J. Cell. Comp. Physiol.* 64:73.

STILLMAN, I. M., D. L. GILBERT, and R. J. LIPICKY. 1971. Effect of external pH upon the voltage-dependent currents of the squid giant axon. *Biophys. Soc. Annu. Meet. Abstr.* 10:55.

WOODBURY, J. W. 1971. Eyring rate theory model of the current-voltage relationships of ion channels in excitable membranes. *In* Chemical Dynamics: Papers in Honor of Henry Eyring. J. O. Hirschfelder and D. Henderson, editors. John Wiley & Sons, Inc., New York.

WOODHULL, A. M. 1972. Ionic blockage of sodium permeability in voltage clamped frog nerve. Doctoral dissertation. University of Washington, Seattle. University Microfilms, Inc., Ann Arbor, Michigan.